Pakistan Jouranal of Information and Technology, 2 (2): 178-190, 2003
ISSN 1682-6027

Morphological Analysis of Mammograms Using Visualization Pipelines

Sabah Mohammed, Jinan Fiaidhi and Lei Yang
Department of Computer Science, Lakehead University,
955 Oliver Road, Thunder Bay, Ontario P7B 5E1, Canada

Abstract: The aim of this study is to detect masses in mammograms through pipelining sequences of visualization operators. Such sequences act as morphological filtering operators for identifying objects of interest. This is done using series of rendering operators including edge detection, smoothing, filling small holes, coloring various densities, joining broken boundaries and eliminating small projections.

Key words: Volume visualization, image morphology, edge detection, mammography

Introduction

Mammography is an effective imaging modality for early breast cancer detection (Caseldine *et al*., 1988 and Tab and Dean, 1987). Despite the advances in mammography, human interpretation still remains very difficult. An estimate of about 10 to 30% of tumors are missed during human interpretation and about 40% of the missed tumors appear as masses (Petrick *et al*., 1996). Several Computer aided diagnosis techniques has been proposed but none is reporting general success (Anguh and Silva, 1997). Spectrum of techniques are under that umbrella including techniques such as edge detection and extraction (Bankman *et al*., 1994; Brzakovic *et al*., 1990), wavelet transforms (Laine *et al*., 1994), neural networks (Bankman *et al*., 1994), filtering (Petrick *et al*., 1996), edge enhancement (Tahoces *et al*., 1987), microcalcification segmentation (Dengler *et al*., 1993) and image classification (Shen *et al*., 1994 and Thiran and Macq, 1980). One of the most important steps in digital mammography is an adequate segmentation of possible tumors. This obviously minimizes errors in further stages such as in classification. However, several factors, some of which are listed below affect the proper segmentation of mammograms. Mammograms contain low signal to noise ratio (low contrast) and a complicated structured background. Breast tissue contrast and density vary with age, thus mammography produces varying image qualities. In addition, mammographic images are not bimodal. As a result, any segmentation method which utilizes an a-priori or single threshold value method is highly likely to generate serious segmentation errors. Moreover, tumors or calcifications are embedded in an inhomogeneous background. In mammograms, background objects may even appear brighter. Therefore, global threshold methods suffer considerable drawback. Adaptive neighbourhood segmentation methods attempt to overcome such drawbacks, but implementational issues such as neighbourhood sizes and the determination of regions where background objects are brighter still pose a difficult problem. These problems can be resolved by considering range of likely thresholds and using pipeline sequences of convolution kernels.

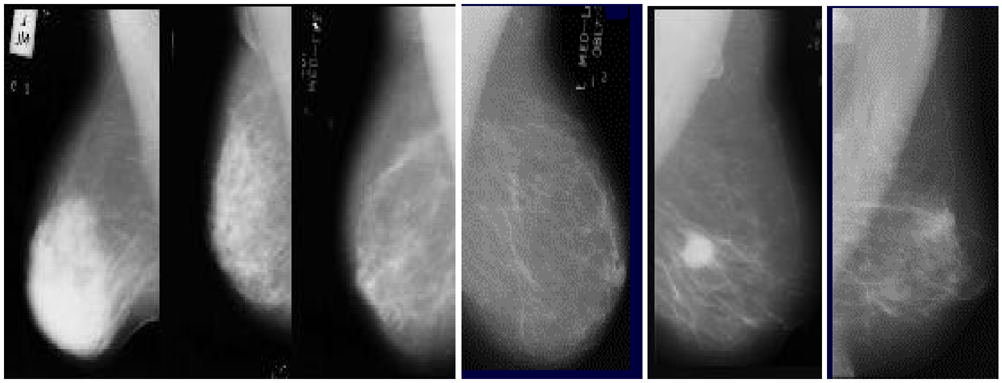

Lipoma Fibroadenomas Normal Calicification Circumscribed Stellate

Fig. 1: Different Abnormalities within mammograms

Searching for the presence of abnormalities in mammographic data is an important step in the detection and diagnosis of breast cancer and other breast illnesses. There are many abnormal shapes that we may encounter when analyzing mammograms. Some of these abnormalities represent harmless regions such as Lipoma (i.e. fatty regions) and Hylanizing Fibroadenomas(i.e. dense fiber area). However, other abnormalities such as stellate lesions, Circumscribed masses and Calcification clusters may represent suspected cases of breast cancer. Fig. 1 illustrates these different breast abnormalities.

All such breast abnormalities can be classified from the region's morphology. This article aims at developing hybrid techniques for identifying the breast morphology using sequences of visualization operators or pipelines.

Morphological analysis techniques

When research into image processing of mammograms began, the preprocessing step was the only enhancement carried out on the image. In more recent years an extra step has been added to most enhancement methods which has led to more accurate shape detection of early tumors. The additional steps includes wide image processing techniques based on Convolution, Thresholding and Mathematical Morphology. In this section we examine their basic effects on breast abnormalities visualization.

Convolution operators

Convolution is a mathematical operation that is fundamental to many common image processing processes. Convolution provides a mechanism for edge detection through 'multiplying together' two arrays of numbers to produce a third array of numbers of the same dimensionality. This can be used in image processing to implement operators whose output pixel values are simple linear combinations of certain input pixel values. In an image-processing context, one of the input arrays is normally a image. The second array is usually much smaller and is also two-dimensional and is known as the kernel. Fig. 2 shows an example image and kernel that we will use to illustrate convolution.

I_{00}	I_{01}	I_{02}	I_{03}	I_{04}	I_{05}	I_{06}	I_{07}	I_{08}
I_{10}	I_{11}	I_{12}	I_{13}	I_{14}	I_{15}	I_{16}	I_{17}	I_{18}
I_{20}	I_{21}	I_{22}	I_{23}	I_{24}	I_{25}	I_{26}	I_{27}	I_{28}
I_{30}	I_{31}	I_{32}	I_{33}	I_{34}	I_{35}	I_{36}	I_{37}	I_{38}
I_{40}	I_{41}	I_{42}	I_{43}	I_{44}	I_{45}	I_{46}	I_{47}	I_{48}
I_{50}	I_{51}	I_{52}	I_{53}	I_{54}	I_{55}	I_{56}	I_{57}	I_{58}
I_{60}	I_{61}	I_{62}	I_{63}	I_{64}	I_{65}	I_{66}	I_{67}	I_{68}
I_{70}	I_{71}	I_{72}	I_{73}	I_{74}	I_{75}	I_{76}	I_{77}	I_{78}

K_{00}	K01	K_{02}
K_{10}	K_{11}	K_{12}
K_{20}	K_{21}	K_{22}

Fig. 2: Convolution Process requires an Image and a Kernel

The convolution is performed by sliding the kernel over the image, generally starting at the top left corner, so as to move the kernel through all the positions where the kernel fits entirely within the boundaries of the image. Each kernel position corresponds to a single output pixel, the value of which is calculated by multiplying together the kernel value and the underlying image pixel value for each of the cells in the kernel and then adding all these numbers together (Batchelor 1993). Fig. 3 illustrates this operation. Using convolution the value of the output pixel O_{22} can be calculated as follows:

$O_{22}=I_{11}*K_{00}+I_{12}*K_{01}+I_{13}*K_{02}+I_{21}*K_{10}+I_{22}*K_{11}+I_{23}*K_{12}+I_{32}*K_{20}+I_{32}*K_{21}+I_{33}*K_{22}$

The roberts cross

Operator performs a simple, quick to compute, 2-D spatial gradient measurement on an image. The operator consists of a pair of 2×2 convolution kernels. One kernel is the other rotated by 90E.

G_x: 1, 0 G_y: 0, 1 $|G|=|G_x|+|G_y|$
0,-1 -1, 0

These kernels are designed to respond maximally to edges running at 45° to the pixel grid, one kernel for each of the two perpendicular orientations. We can see that the result image is very dark when applying the Roberts Cross operator to mammogram.

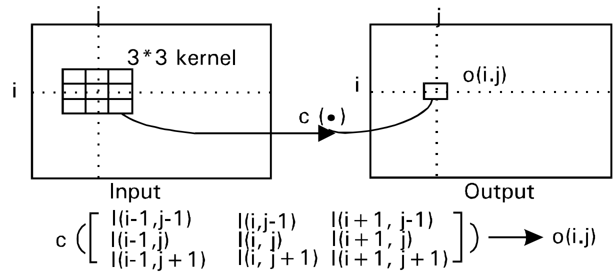

Fig. 3: Illustrating the Process of Convolution. The convolution process is a highly researched issue and it is affected by many factors. Basic to all is the kernel type being used and the size of the kernel. There are many types of kernels had been proposed in the literature (Gonzalez and Woods 2002) and basic to all are the following kernel types

Laplacian

Is a 2-D isotropic measure of the 2nd spatial derivative of an image. The Laplacian of an image highlights regions of rapid intensity change and is therefore often used for edge detection.

-1,-1,-1		-1,- 4, -1.
-1, 8,-1	or	-4,20,-4
-1,-1,-1		-1,-4, -1

Sobel

Operator performs a 2-D spatial gradient measurement on an image and so emphasizes regions of high spatial frequency that correspond to edges. Typically it is used to find the approximate absolute gradient magnitude at each point in an input image. Sobel Kernels are:

-1, 0, 1,		-1,-2,-1,
-2, 0, 2	and	0, 0, 0,
-1, 0, 1,		1, 2, 1,

These kernels are designed to respond maximally to edges running vertically and horizontally relative to the pixel grid, one kernel for each of the two perpendicular orientations. The kernels can be applied separately to the input image, to produce separate measurements of the gradient component in each orientation (call these G_x and G_y). These can then be combined together to find the absolute magnitude of the gradient at each point $|G| = \sqrt{Gx^2 + Gy^2}$ and the orientation of that gradient. An approximate magnitude can be computed using: $|G|=|G_x|+|G_y|$.

Compass

Edge Detection is an alternative approach to the differential gradient edge detection. When using compass edge detection the image is convoluted with a set of (in general 8) convolution kernels, each of which is sensitive to edges in a different orientation. For each pixel the local edge gradient magnitude is estimated with the maximum response of all 8 kernels at this pixel location:

$$|G| = max\left(|G_i| : i = 1\ to\ n\right)$$

where G_i is the response of the kernel i at the particular pixel position and n is the number of convolution kernels. The local edge orientation is estimated with the orientation of the kernel that yields the maximum response. Various kernels can be used for this purpose; and best of all are the Prewitt and the Kirsch kernels. Two templates out of the set of 8 are shown below:

0^0:-1, 1, 1 45^0: 1, 1, 1
-1,-2, 1   -1,-2, 1
-1, 1, 1   -1,-2, 1

Kirsch

Edge Detector (Parker, 1997) is another compass kernel. The masks given by these templates try to model the kind of grey level change seen near an edge having various orientations. There is a mask for each of eight compass directions. For instance K0 implies a vertical edge (horizontal gradient) at the pixel corresponding at the center of the mask. To find the edge, I is convolved with the eight masks at each pixel position. The response is the maximum of the responses of any of the eight masks and the directions quantified into eight possibilities.

K0: -3,-3, 5   K1: -3, 5, 5   ……
-3, 0, 5   -3, 0, 5
-3,-3, 5   -3,-3,-3

The effects of using these kernels on mammogram's tumor detection vary so much as Fig. 4 illustrates. The experiment shows that Kirsch and Sobel kernels have better detection power from the other kernels.

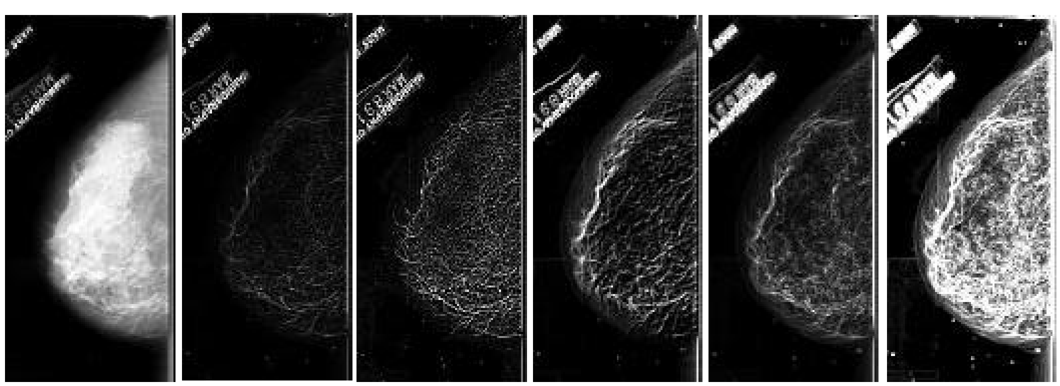

Original Image   Roberts Cross   Laplacian   Sobel   Prewitt Compass   Kirsch Compass

Fig. 4: The effects of different kernel types on breast tumor's detection

Kernel size can affect the resolution power of the convolution processes. It can increase the thickness of the edge detected. Fig. 5 illustrate the results of another experiment conducted using the Laplacian Kernel and varying its size from 3x3 to 9x9. That is why most of the researchers uses 3x3 or 5x5 kernel size avoiding over or under resolution.

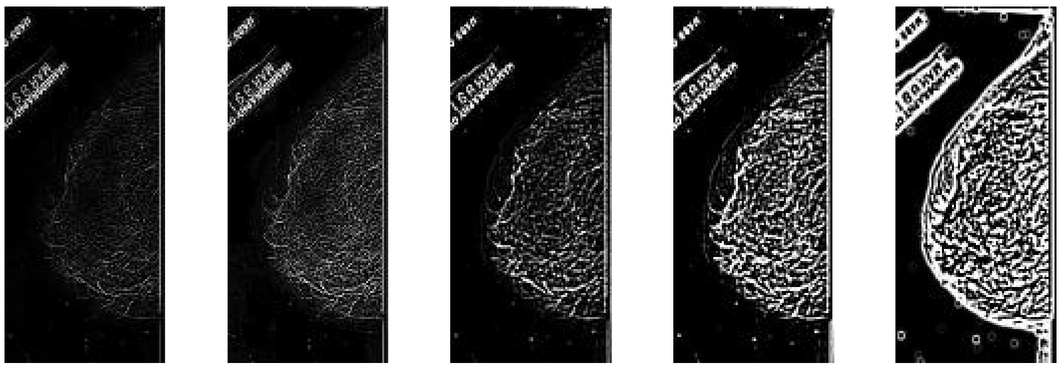

(0, 18, 255) (0,138,255) (0, 160, 255) (0, 216, 255) (0, 240, 255)

Fig. 5: Effects of the Kernel Size on the Convolution Resolution

Thresholding operators

Threshold makes color changes across a programmer-determined boundary, or threshold, more obvious. This technique uses a specified threshold value, minimum value and maximum value to control the color component values for each pixel of an image. Color values below the threshold are assigned the minimum value. Values above the threshold are assigned the maximum value. The threshold process is performed for each color component of each pixel. When the operation is complete, the color components of the destination image pixels will contain either the minimum value or the maximum value. For example, consider what happens to an image when a threshold operation is performed with a minimum of 0 and a maximum of 255. After the image is processed, the red, green and blue values of the pixels will be either 0 or 255. In the following examples, we write threshold value in (min, threshold, max) format. We can see that the white area (indicate the higher brightness area) getting smaller with the threshold value go up. Thresholding is very important morphological technique for detecting tumor regions because a tumor represent a dense tissue area of the breast structure. However, it very tricky to find the right threshold value that can work for variety of mammograms. For this purpose many researchers tried to arrive at a dynamic threshold which can learn its optimal value from the type of image under analysis. Fig. 6 illustrates the effects of using variety of static thresholds.

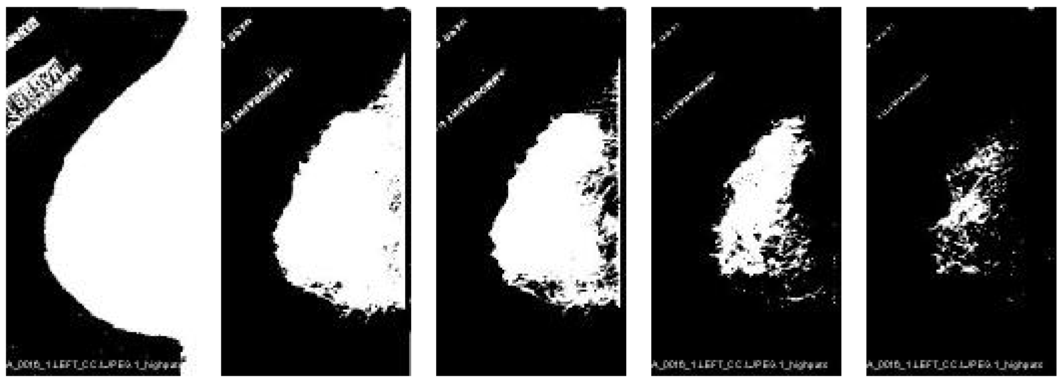

3*3 Kernel 3*3 Kernel 5*5 Kernel 7*7 Kernel 9*9 Kernel

Fig. 6: Effects of various static thresholds

Mathematical morphology operators

Morphological operators often take a binary image and a structuring element as input and combine them using a set operator (intersection, union, inclusion, complement). For the basic morphological operators the structuring element contains only foreground pixels (i.e. ones) and `don't care's'. These operators, which are all a combination of erosion and dilation, are often used to select or suppress features of a certain shape, e.g. removing noise from images, skeletonization-thinning or selecting objects with a particular direction. Morphological operators can also be applied to gray-level images, e.g. to reduce noise or to brighten the image. The method is to treat the image as a sequence of binary images by operating on each gray level as if it were the 1 value and assuming everything else to be 0. The resulting images can then be combined by laying them on top of each other and "promoting" each pixel to the highest gray-level value coincident with that location. Mathematical morphology provides a number of important image processing operations, including erosion, dilation, opening and closing.

Erosion

The basic effect of the operator on a binary image is to erode away the boundaries of regions of foreground pixels (i.e. white pixels, typically). Thus areas of foreground pixels shrink in size and holes within those areas become larger. To compute the erosion of a binary input image by this structuring element, we consider each of the foreground pixels in the input image in turn. For each foreground pixel (which we will call the input pixel) we superimpose the structuring element on top of the input image so that the origin of the structuring element coincides with the input pixel coordinates. If for every pixel in the structuring element, the corresponding pixel in the image underneath is a foreground pixel, then the input pixel is left as it is. If any of the corresponding pixels in the image are background however, the input pixel is also set to background value.

Dilation

The basic effect of Dilation operator on a binary image is to gradually enlarge the boundaries of regions of foreground pixels. Thus areas of foreground pixels grow in size while holes within those regions become smaller.

Opening and closing are both derived from the fundamental operations of erosion and dilation. The basic effect of an opening is somewhat like erosion in that it tends to remove some of the foreground (bright) pixels from the edges of regions of foreground pixels. However it is less destructive than erosion in general. As with other morphological operators, the exact operation is determined by a structuring element. The effect of the operator is to preserve foreground regions that have a similar shape to this structuring element, or that can completely contain the structuring element, while eliminating all other regions of foreground pixels. Closing is similar in some ways to dilation in that it tends to enlarge the boundaries of foreground (bright) regions in an image (and shrink background color holes in such regions), but it is less destructive of the original boundary shape. Fig. 7 illustrates the effects of applying repetitive erosion and dilation operators on mammograms. It is obvious that erosion aims at thinning the region while dilations reduce the noise within the image regions. The opening and closing operations have no obvious effects on the mammograms. The structuring element used in these experiments is 3x3 matrix with all elements equal to 1.

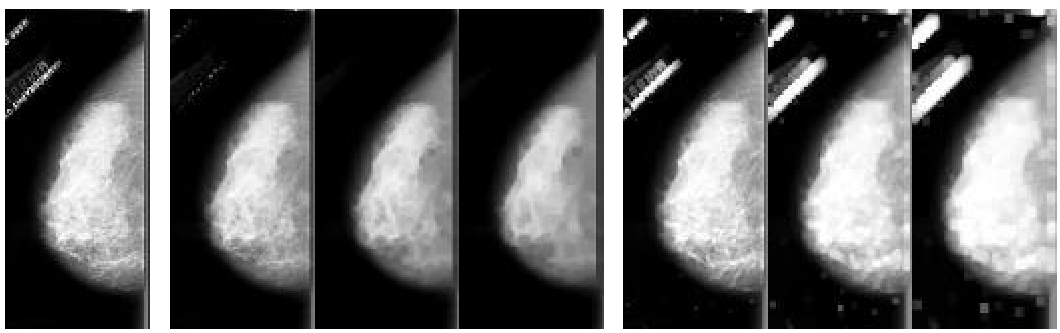

Original Erosion 1 time 3 times 5 times Dilation 1 time 3 times 5 times

Fig. 7: The effects f Applying three times the Erosion and Dilation Operators

Visualization pipelines

Usually research in volume visualization (Elvins, 1992) is used to create images from scalar and vector datasets defined on multiple dimensional grids, i.e., it is the process of projecting a multidimensional (usually 3D) dataset onto a 2D image stack to gain an understanding of the structure contained within the data. After the image stack is processed by 2-D image processing techniques, it can then be reconstructed into either a 3-D volumetric dataset or a rendered 2D image. This is a new but rapidly growing field in both computer graphics and data visualization (Bredlie and Wood, 2001). These techniques are used in medicine, geoscience, astrophysics, chemistry, microscopy, mechanical engineering and other areas. Visualization is usually achieved using either volume or surface rendering techniques.

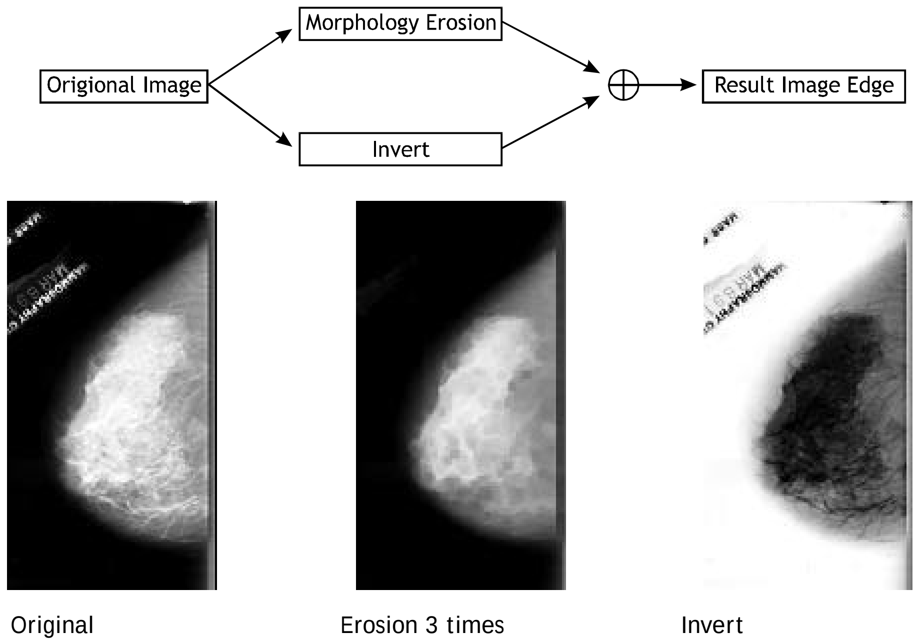

Fig. 8: Simple Visualization Pipleline

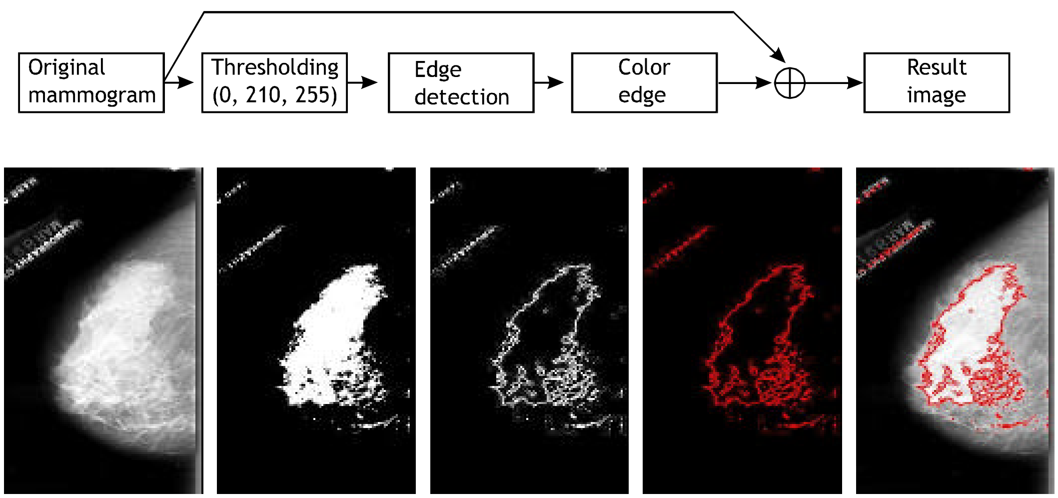

Fig. 9: Visualization Pipeline aiming at separating the image into high and low brightness areas

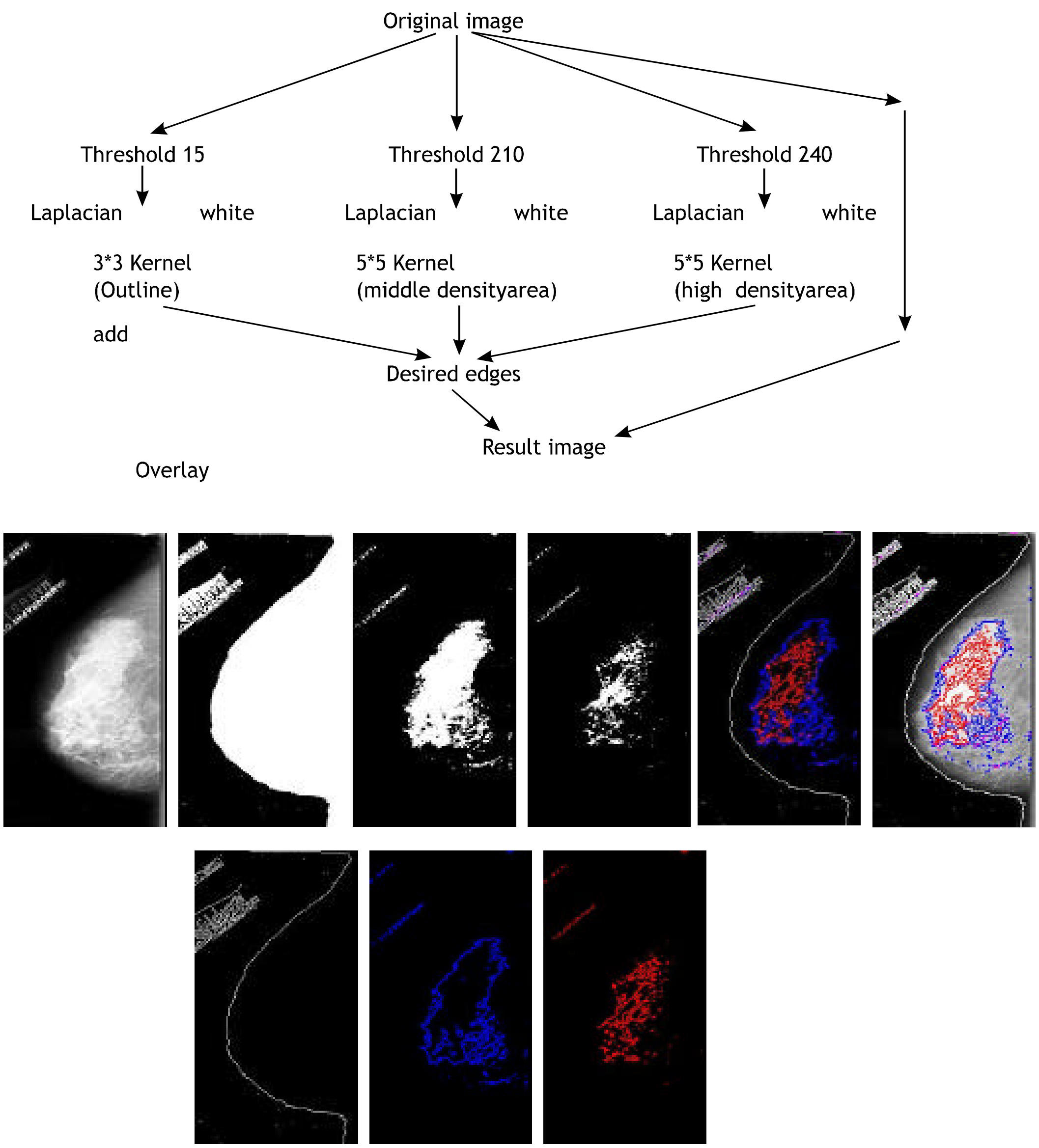

Fig. 10: Visualization Pipelines for separating different lightness areas

Volume rendering is a computer graphics technique whereby the object or phenomenon of interest is sampled or subdivided into many cubic building blocks, called volume elements. Each volume element can be treated separately.

The resulted volume elements can be assembled from multiple 2-D images (i.e. image stack) and are displayed by projecting these images into either 2-D pixel space or storing them as frames for 3D projection.

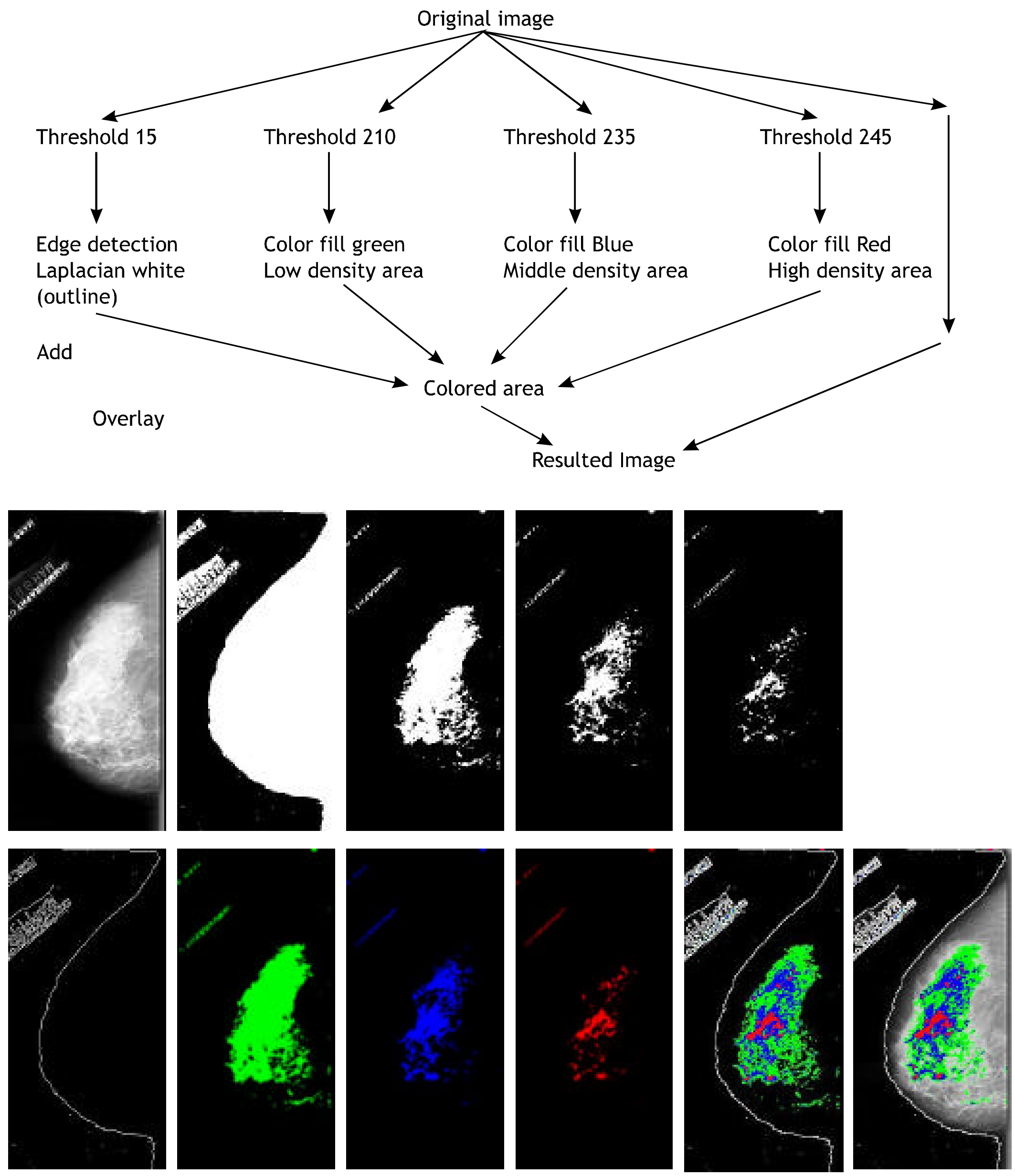

Fig. 11: Visualization Pipeline with Area Filling Rendering Effects

In surface rendering, the volumetric data must first be converted into geometric primitives, by a process such as isosurfacing, isocontouring, surface extraction or border following. These primitives (such as polygon meshes or contours) are then rendered for display using conventional geometric rendering techniques.

Both techniques have advantages and pitfalls. A major advantage of the volume rendering technique is that the image data volume can be displayed without any knowledge of the geometry of the dataset and hence without intermediate conversion to a surface representation. This conversion step in surface rendering can sometimes be quite complex, especially if surfaces are not well defined (i.e. noisy 2-D images) and can require a lot of user intervention (such as manual contour tracing)

In this section we are proposing certain pipelines for mammograms volume visualization. Such visualization pipelines are based on the proper choice of various morphological transfer operators in order to map the original image data into meaningful optical properties of the volume to be visualized. The transfer operators represents basic segmentation methods (e.g convolution, thresholding) as well as other binary operators such as add, subtract, invert, overlay, erosion and dilation.

The visualization pipelines can be simple when the rendered image it is composed of using only binary operations such as erosion and inversion (Fig. 8).

More complex visualization pipelines can be produced when edge detection operators are involved. Fig. 9 illustrates our first expirement when the we used a thresholding value of (210) to segment the image into high brightness and low brightness areas.

We can use more than one threshold value to highlight the various volume elements in the image as Fig. 10 illustrates:

We can enhance the rendered areas by filling the segmented areas by different colors. Fig. 11 illustrates the new visualization pipelines.

Physicians and clinical researchers seeking new tools in their escalating war against cancer could use a new rendering technique for identifying the morphological structure of mammograms, a process that will help them learn more about patients at high risk for developing breast cancer. Morphological analysis of mammograms requires very careful visualization techniques. Such techniques can aid the process of the automatic detection of the various breast abnormalities and illnesses. This project proposes the use of various visualization operators for volume visualization of mammograms. Conducted experiments suggest its affectivity. The next step is to try to use these visualization operators on proven cancer cases from sound Medical Databases such as the mammography database for the mammographic Image Society (See http://www.wiau.man.ac.uk/services/MIAS/MIASmini.html) and the Digital Database for Screening Mammography (DDSM) (See http://marathon.csee.usf.edu/Mammography/Database.html). This step is left for our future research work.

References

Anguh M. and A. Silva, 1997. Multiscale Segmentation and Enhancement in Mammograms, The 6th Brazilian Image Processing Symposium SIBGRAPI' 97,, SP, Brazil, pp: 14-17.

Bankman *et al*., 1994 Detection of Microcalcification Clusters Using Neural Networks, IEEE, pp: 590-591.

Bredlie K. and J. Wood, 2001. Recent Advances in Volume Visualization, Computer Graphics Forum, 20: 2.

Bruce Batchelor and Frederick Waltz, 1993. Interactive Image Processing for Machine Vision, Springer Verlag, New York.

Brzakovic *et al*., 1990. An Approach to Automate Detection of Tumors in Mammograms, IEEE Trans. Medical Imaging, 9: 233-241.

Caseldine, J., R. Blamey, E. Roebuck and C. Elston, 1988. Breast Disease for Radiographers,Wright.

Dengler *et al*., 1993. Segmentation of Microcalcification in Mammograms, IEEE Trans. Medical Imaging, 12: 634-642.

Elvins, T., 1992. Survey of Algorithms for Volume Visualization, Computer Graphics, 26: 194-201.

Gonzalez, R. and R. Woods, 2002. Digital Image Processing, 2nd Ed. Addison-Wesley, 2002.

Laine *et al*., 1994. Mammographic Feature Enhancement by Multiscale Analysis, IEEE Trans. Medical Imaging, 13: 725-738.

Parker, J.R., 1997. Algorithms for Image Processing and Computer Vision, Wiley Computer Publishing.

Petrick *et al*., 1996. An Adaptive Density-Weighted Contrast Enhancement Filter for Mammographic Breast Mass Detection, IEEE Trans. Medical Imaging, 15: 59-67.

Shen *et al*., 1994. Application of Shape Analysis to Mammographic Calcification, IEEE Trans. Medical Imaging, 13: 263-274.

Tabar, L. and P.B. Dean, 1987. The Control of Breast Cancer through Mammography Screening: What is the Evidence, Radiol. Clin. N. Amer., 25: 993-1005.

Tahoces *et al*., 1991. Enhancement of Chest andBrest Radiographs by Autimatic Spatial Filtering, IEEE Trans. Medical Imaging, 10: 330-335.

Thiran J.P. and B. Macq, 1980. Morphological Feature Extraction for the Classification of Digital Images of Cancerous Tissues, IEEE Trans. on Biomedical Engineering, 43: 1011-1020.